XXXIII Congresso Brasileiro de Ciência do Solo
Solos nos biomas brasileiros: sustentabilidade e mudanças climáticas
31 de julho à 05 de agosto - Center Convention - Uberlândia/Minas Gerais

MAPPING OF SOIL CLASSES IN A COMPLEX TROPICAL ENVIRONMENT ENHANCED BY STREAM DENSITY AND LABORATORY SPECTROSCOPY

Gustavo de Mattos Vasques[(1)]; José Alexandre Melo Demattê[(2)]; Raphael Viscarra Rossel[(3)]; Leonardo Ramírez López[(4)]; Fabrício da Silva Terra[(2)]; Rodnei Rizzo[(2)]

[(1)] Researcher; Embrapa Solos, Rua Jardim Botânico, 1024, Rio de Janeiro, RJ, 22460-000, Brazil; gustavo@cnps.embrapa.br; [(2)] Professor; Student; Student; Departamento de Ciência do Solo, Universidade de São Paulo, Av. Pádua Dias 11, Caixa Postal 9, Piracicaba, SP, 13418-900, Brazil; [(3)] Researcher; Christian Laboratory, CSIRO Land and Water, Clunies Ross Street, Black Mountain, ACT 2601, GPO Box 1666, Canberra, Australia; [(4)] Student; Geographisches Institut, Universität Tübingen, Rümelinstraße 19-23, 72070, Tübingen, Germany

Abstract – There is need to integrate methods to enhance soil maps across large areas. This study proposes a novel and simple method to incorporate laboratory soil spectral data in the production of a digital soil map. We integrated laboratory, field and remote sensing data to derive a map of soil suborder based on the Brazilian Soil Classification System. We described and classified 289 soil profiles in an area of ~13,000 ha with great soil, geologic, and topographic variation in the state of São Paulo, southeastern Brazil. Multinomial logistic regression was used to classify soils based on geospatial data (geology, topography, emissivity, vegetation index, and land cover), and laboratory soil visible/near-infrared (400-2500 nm) reflectance at three depths (0-20, 40-60, and 80-100 cm). Soil suborders were correctly classified in 52% of the cases, and agreed with a 1:100,000, and a 1:20,000 reference conventional map in 41, and 46% of the area, respectively. Stream density and laboratory soil reflectance were included in, and improved, suborder classification models, showing great potential to aid digital soil mapping in complex environments.

Keywords: digital soil mapping, multivariate classification, pedometrics, soil-landscape modeling

INTRODUCTION

Soil survey involves costly and time-consuming office, laboratory and field work to collect, characterize, classify, and map soils. This approach hampers the update of maps, and can lead to inaccurate delineation of soil boundaries, especially when interpreting many factors simultaneously.

Offering a spatially explicit approach to soil survey, digital soil mapping (DSM) has gradually incorporated new sensors, models, and digital data, aiming to improve accuracy and cost of soil survey. Many studies have used geospatial data (e.g. topography, satellite imagery) to produce soil attribute maps (e.g. Cook et al., 1996; Breunig et al., 2009; Vasques et al., 2010), and less commonly soil class maps (e.g. Dobos et al., 2000; Demattê et al., 2005; Hengl et al., 2007). However, proximally sensed (laboratory or field) spectral data have modestly been used for soil taxonomic classification (Du et al., 2008), and rarely to produce maps (Viscarra Rossel & Chen, 2011). Thus, integrating proximal (spectroscopy) and remote sensing data for DSM is greatly needed.

The objectives of this study were to: (i) derive a soil suborder map using DSM based on geospatial (GIS), field, and laboratory spectral data; and (ii) compare the derived map with conventional soil survey maps at two scales.

MATERIALS AND METHODS

Study area, soil sampling and analysis

The 13,000-ha study area is located in the central-eastern portion of the state of São Paulo, Brazil (Figure 1), and has been used for sugarcane production in the last 30 years. Mean annual precipitation, and temperature are 1328 mm, and 21.6 ºC, respectively. Geologically, soils in the area have predominantly formed from sandstone, siltstone, and shale, and less so from limestone, basalt, and colluvial deposits (Mezzalira, 1966). Elevations vary from about 489 to 709 m, and slopes from 0 to 32%.

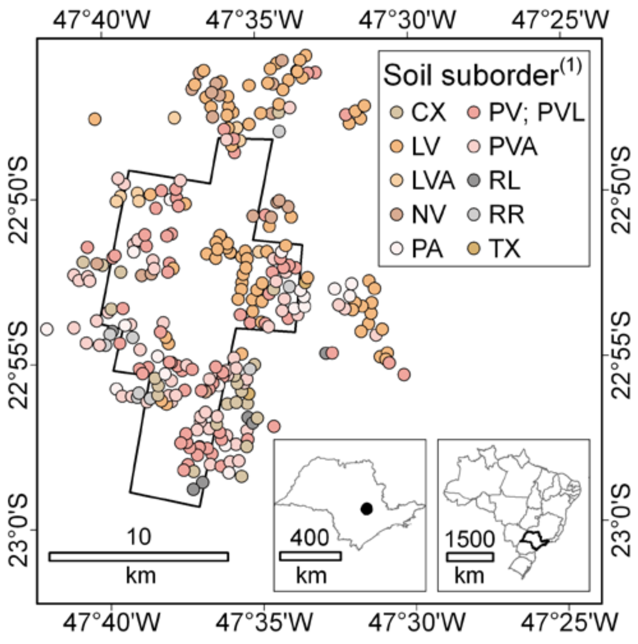

Figure 1. Study area, and sampling design, showing soil suborders as classified in the field

[(1)] Soil suborders and corresponding soil classes in Soil Taxonomy (Soil Survey Staff, 2010): CX, Cambissolo Háplico – Udepts; LV, Latossolo Vermelho, LVA, Latossolo Vermelho-Amarelo – Udox; NV, Nitossolo Vermelho, PA, Argissolo Amarelo, PV, Argissolo Vermelho, PVA, Argissolo Vermelho-Amarelo, PVL, Argissolo Vermelho Latossólico – Udalfs, Udults; RL, Neossolo Litólico – Lithic Udorthents, Lithic Udipsamments; RR, Neossolo Regolítico – Udorthents, Udipsamments; TX, Luvissolo Háplico – Udalfs

A total of 289 soil profiles (11 pits, and 278 boreholes; Figure 1) were visited and classified in the field at the suborder level (second highest) according to the Brazilian Soil Classification System (SiBCS; EMBRAPA, 2006). Soil samples were taken at 0-20, 40-60, and 80-100 cm, and analyzed chemically and granulometrically according to Camargo et al. (1986).

Soil reflectance spectra in the visible/near-infrared (VNIR; 400-2500 nm) were collected in the laboratory from air-dried and sieved (2 mm) samples using a FieldSpec Pro sensor (Analytical Spectral Devices Inc., Boulder, CO), 100 scans per sample, and Spectralon (Labsphere, North Sutton, NH) as white reference. For each soil profile, at each depth interval, a soil spectral curve was collected, and an average reflectance value across the spectrum calculated for use in the models.

Soil suborder modeling and mapping

The following GIS layers were prepared with 30-m resolution for use in the models: (1) stream density (SD) as the total length of streams per unit area within a radius of 750 m (streams were delineated from 1:30,000 aerial photographs using a stereoscope); (2) elevation, and nine topographic attributes (slope; flow accumulation; aspect; wetness, sediment, and power indices; and plan, profile, and mean curvatures) derived from 90-m Shuttle Radar Topography Mission digital elevation model; (3) geologic units digitized from a 1:100,000 map (Mezzalira, 1966); five emissivity bands (10 through 14), and normalized different vegetation index derived from Terra/Aster imagery; (4) land cover derived from Aster imagery using supervised classification by maximum likelihood; and (5) average soil reflectance at three depths interpolated across the study area using splines.

Multinomial logistic regression (MLR; Agresti, 2002) was used to classify the soil observations into suborders using the environmental GIS layers as independent variables. The independent GIS variables were divided into five groups (Table 1), and models were derived using stepwise selection (p-value = 0.05) of *Geomorphic* variables alone, or combinations of *Geomorphic* and other variable groups.

In MLR, the model predicts the probability of the observation belonging to each possible categorical response (i.e. soil class) based on the selected predictors. To produce the soil suborder map, the MLR model with the highest agreement rate was used, and each pixel received the value of the suborder with the highest probability of occurrence. To minimize an undesirable 'salt and pepper' effect, a majority filter (3x3 moving window) was applied in the classified soil map with 50 successive passes.

Comparison among digital and conventional maps

The digital suborder map derived in this study was compared to two maps produced using conventional soil survey methods, one at 1:100,000 (Oliveira & Prado, 1989), and another at 1:20,000, created by the authors of this study. The percent of agreement was calculated on an areal basis for two maps at a time based on their superimposed intersection areas.

RESULTS AND DISCUSSION

Soil suborder modeling and mapping

The MLR models classified soil suborders correctly in 43 to 52% of the cases (Table 2), with the best model including *Geomorphic* + *Spectral* variables (slope; stream density; and average soil reflectance at 0-20, and 40-60 cm). The resulting map (Figure 2) shows predominance of PV (35% of the area), followed by LV (33%), and PVA (29%) in the area.

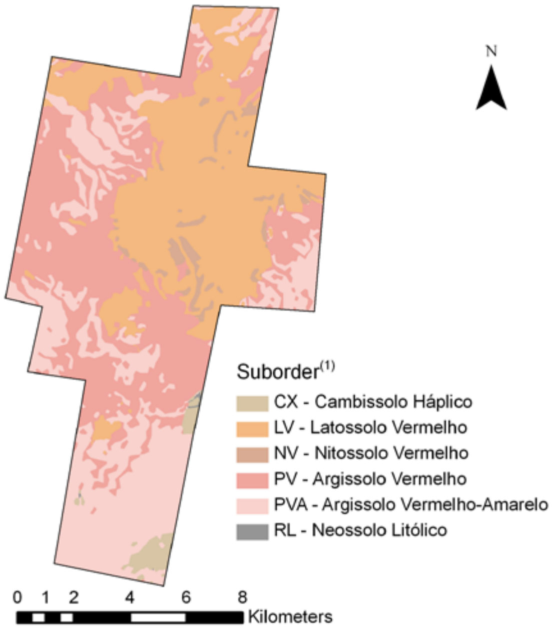

Figure 2. Predicted map of soil suborder based on the best multinomial logistic model using *Geomorphic* and *Spectral* variables

(1) Corresponding soil classes in Soil Taxonomy (Soil Survey Staff, 2010): CX – Udepts; LV – Udox; NV, PV, PVA – Udalfs, Udults; RL – Lithic Udorthents, Lithic Udipsamments

Stream density (Figure 3) was consistently selected by all MLR models. Since it conveys information about the drainage pattern around the soil, it is directly linked to processes of soil formation that involve the movement of water. These processes were, in turn, considered in the very conception and delineation of soil classes in the SiBCS (EMBRAPA, 2006), which explains the remarkable similarity between the soil suborder, and SD maps. For example, LV – deep, hematite-rich soils – tended to occur in oxidizing environments in more stable, upper and drier positions with smaller SD. In contrast, PVA – shallower, yellower soils with an argillic horizon – occurred in more humid positions with higher SD, as expected (Macedo & Bryant, 1987; Schwertmann, 1988). Argissolo Vermelho occurred in intermediate positions (medium SD).

In a related study in Rio Grande do Sul, southern Brazil, Figueiredo et al. (2008) correlated soil mapping units at the great group level (third highest) from a

1:80,000 conventional soil map with terrain attributes to build predictive logistic models, obtaining 58% agreement. Also in Rio Grande do Sul, ten Caten (2008) used a 1:50,000 conventional soil map to train a MLR model to predict soil suborder, obtaining an overall 60% agreement rate.

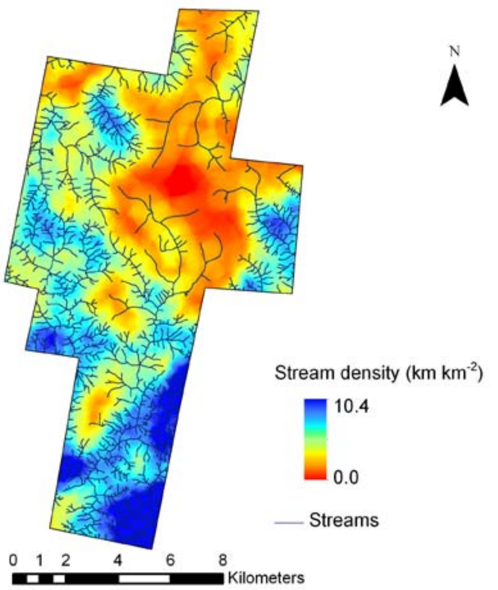

Figure 3. Stream network, and stream density within a 750-m radius

In these studies, it was assumed that the conventional soil maps represented ground truth and that digital soil maps should portray soil-landscape relationships as perceived by the soil surveyor. In contrast, our model was built based on statistical relationships among visited soil profiles and co-located landscape attributes. Thus, in our study soil mapping unit boundaries were defined based on statistical limits in soil-landscape relationships, as opposed to the other studies that considered soil boundaries as delineated by the surveyor based on expert knowledge.

In this sense, our study was more similar to Hengl et al. (2007), and Mendonça-Santos et al. (2008). In the former, different interpolation methods (including MLR) were compared to map soil classes in Iran, obtaining contrasting results among methods, which were attributed to the similarity among soil classes in the feature space, and the quality of soil-landscape correlations. In the latter, classification trees were applied to predict soil orders in Rio de Janeiro, Brazil, based on 431 observations, obtaining agreement rates of 54 to 96% in validation.

Soil classification models were also improved with the addition of laboratory soil reflectance at multiple depths, complementing the geospatial data included in the models. Soil VNIR reflectance not only conveys soil color – an important criterion to classify soils at the suborder level in the SiBCS (EMBRAPA, 2006) – but also relates to various soil constituents, including organic matter, water, and iron, to name a few (e.g. Demattê et al., 2003; Viscarra Rossel et al., 2006).

A few examples where laboratory soil spectroscopy was directly used in DSM include Wetterlind et al. (2008), who used VNIR spectroscopy to predict soil organic matter and clay content to augment a soil dataset for precision agriculture, and Gomez et al. (2008), who used mid-infrared spectroscopy as the 'standard' method to estimate soil organic carbon, which was then used to calibrate soil organic carbon models based on field, and remote (Hyperion) VNIR reflectance, respectively. Rather than substituting wet chemistry, our aim was to augment the pool of environmental variables to predict soil suborder with a relatively cheap and easy-to-measure soil property.

Comparison among digital and conventional maps

The soil suborder digital map agreed with the 1:100,000, and 1:20,000 conventional maps (not shown) in 41, and 46% of the area, respectively. Compared to the conventional maps, mapping units in the digital map were generally more complex, and more intermixed. The digital map distinguished LV from Latossolo Vermelho Férrico (LVF, Udox), which was only possible based on their spectral reflectance, and also provided alternative boundaries among Latossolo (Oxisols) suborders (LV, LVA, and LVF), Argissolo (Ultisols) suborders (PA, PV, PVA, PVF, and PVL), and among LV, PV and PVA, the commonest suborders in the area (Figure 2).

The digital map also distinguished areas of Neossolo (RL, and RR; Entisols), Cambissolo (CX; Inceptisols), and Argissolo (PA, PV, PVA, PVF, and PVL; Ultisols) based on the slope, and SD, with Neossolos occupying steeper and higher-SD areas, and Argissolos flatter and smaller-SD areas. Cambissolos occurred on intermediate conditions.

CONCLUSIONS

1. Multinomial logistic regression can accommodate both continuous and categorical environmental predictors, and provide quantitative, interpretable soil suborder-landscape relationships;

1. Including stream density and laboratory soil reflectance in the classification models allows to better separate soils with similar soil-landscape conditions, improving soil classification and mapping.

ACKNOWLEDGEMENTS

We thank the Soil Science Department at the University of São Paulo, the Coordination for the Improvement of Higher Education Personnel (CAPES), the Commonwealth Scientific and Industrial Research Organisation (CSIRO), and the Foundation for Research Support of the State of São Paulo (FAPESP) for the support.

REFERENCES

AGRESTI, A. Categorical data analysis. 2.ed. New York, John Wiley & Sons, 2002. 734p.

BREUNIG, F.M.; GALVÃO, L.S.; FORMAGGIO, A.R. & COUTO, E.G. The combined use of reflectance, emissivity and elevation Aster/Terra data for tropical soil studies. R. Bras. Ci. Solo, 33:1785-1794, 2009.

CAMARGO, O.A.; MONIZ, A.C.; JORGE, J.A. & VALADARES, J.M.A.S. Métodos de análise química, mineralógica e física de solos do Instituto Agronômico de Campinas. Campinas, Instituto Agronômico, 1986. 94p.

COOK, S.E.; CORNER, R.J.; GROVES, P.R. & GREALISH, G.J. Use of airborne gamma radiometric data for soil mapping. Aust. J. Soil Res., 34:183-194, 1996.

DEMATTÊ, J.A.M.; EPIPHANIO, J.C.N. & FORMAGGIO, A.R. Influência da matéria orgânica e de formas de ferro na reflectância de solos tropicais. Bragantia, 62:451-464, 2003.

DEMATTÊ, J.A.M.; MORETI, D.; VASCONCELOS, A.C.F. & GENÚ, A.M. Uso de imagens de satélite na discriminação de solos desenvolvidos de basalto e arenito na região de Paraguaçu Paulista. Pesq. Agrop. Bras., 40:697-706, 2005.

DOBOS, E.; MICHELI, E.; BAUMGARDNER, M.F.; BIEHL, L. & HELT, T. Use of combined digital elevation model and satellite radiometric data for regional soil mapping. Geoderma, 97:367-391, 2000.

DU, C.; LINKER, R. & SHAVIV, A. Identification of agricultural Mediterranean soils using mid-infrared photoacoustic spectroscopy. Geoderma, 143:85-90, 2008.

EMBRAPA (EMPRESA BRASILEIRA DE PESQUISA AGROPECUÁRIA). Sistema Brasileiro de Classificação de Solos. 2.ed. Brasília, EMBRAPA, 2006. 306p.

FIGUEIREDO, S.R.; GIASSON, E.; TORNQUIST, C.G. & NASCIMENTO, P.C. Uso de regressões logísticas múltiplas para mapeamento digital de solos no Planalto Médio do RS. R. Bras. Ci. Solo, 32:2779-2785, 2008.

GOMEZ, C.; VISCARRA ROSSEL, R.A. & MCBRATNEY, A.B. Soil organic carbon prediction by hyperspectral remote sensing and field vis-NIR spectroscopy: an Australian case study. Geoderma, 146:403-411, 2008.

HENGL, T.; TOOMANIAN, N.; REUTER, H.I. & MALAKOUTI, M.J. Methods to interpolate soil categorical variables from profile observations: lessons from Iran. Geoderma, 140:417-427, 2007

MACEDO, J. & BRYANT, R.B. Morphology, mineralogy, and genesis of a hydrosequence of Oxisols in Brazil. Soil Sci. Soc. Am. J., 51:690-698, 1987.

MENDONÇA-SANTOS, M.L.; SANTOS, H.G.; DART, R.O. & PARES, J.G. Digital mapping of soil classes in Rio de Janeiro state, Brazil: data, modelling and prediction. In: HARTEMINK, A.E.; McBRATNEY, A.B. & MENDONÇA-SANTOS, M.L., ed. Digital soil mapping with limited data. Amsterdam, Springer, 2008. p.381-396.

MEZZALIRA, S. Folha geológica de Piracicaba. Folha SF-23-M-300. São Paulo, Instituto Geográfico e Geológico do Estado de São Paulo, 1966.

OLIVEIRA, J.B. & PRADO, H. Carta pedológica semi-detalhada do estado de São Paulo: quadrícula de Piracicaba. Folha SF-23-Y-A-IV. Campinas, Instituto Agronômico, 1989.

SCHWERTMANN, U. Occurrence and formation of iron oxides in various pedoenvironments. In: STUCKY, J.W.; GOODMAN, B.A. & SCHWERTMANN, U., ed. Iron in soils and clay minerals. Dordrecht, D. Reidel, 1988. p.267-308.

SOIL SURVEY STAFF. Keys to Soil Taxonomy. 11.ed. Washington, United States Department of Agriculture, 2010. 338p.

TEN CATEN, A. Aplicação de componentes principais e regressões logísticas múltiplas em sistema de informações geográficas para a predição o e mapeamento digital de solos. Master’s Thesis. Santa Maria, Universidade Federal de Santa Maria, 2008. 128p.

VASQUES, G.M.; GRUNWALD, S.; COMERFORD, N.B. & SICKMAN, J.O. Regional modelling of soil carbon at multiple depths within a subtropical watershed. Geoderma, 156, p.326-336, 2010.

VISCARRA ROSSEL, R.A. & CHEN, C. Digitally mapping the information content of visible–near infrared spectra of surficial Australian soils. Remote Sens. Environ., 115:1443-1455, 2011.

VISCARRA ROSSEL, R.A.; WALVOORT, D.J.J.; MCBRATNEY, A.B.; JANIK, L.J. & SKJEMSTAD, J.O. Visible, near infrared, mid infrared or combined diffuse reflectance spectroscopy for simultaneous assessment of various soil properties. Geoderma, 131:59-75, 2006.

WETTERLIND, J.; STENBERG, B. & SÖDERSTRÖM, M. The use of near infrared (NIR) spectroscopy to improve soil mapping at the farm scale. Precis. Agric., 9:57-69, 2008.

Table 1. Groups of independent variables included in the multinomial logistic models

Group	Number of variables	Description
Geomorphic	11	Elevation; slope; flow accumulation; aspect; wetness, sediment, and power indices; plan, profile, and mean curvatures; stream density
Aster	6	Aster emissivity bands 10 through 14; normalized difference vegetation index
Spectral	3	Average soil reflectance at 0-20, 40-60, and 80-100-cm depths
Geologic	7	Seven geologic classes(1)
Land cover	6	Six land cover classes(2) derived from Aster imagery

(1) Geologic classes included: colluvial deposits; Corumbataí Formation (Fm); Irati Fm; Itararé Subgroup; Piramboia Fm; Serra Geral Fm; and Tatuí Fm. (2) Land cover classes included: exposed sandy soil; exposed medium-textured soil; exposed clayey soil; pasture; sugarcane; and sugarcane residue

Table 2. Soil suborder multinomial logistic classification results from different combinations of independent variable groups

Independent variable groups	Number of selected variables	Agreement rate (%)
Geomorphic	2	42.9
Geomorphic + Aster	2	42.9
Geomorphic + Spectral	4	51.6
Geomorphic + Geologic	5	46.0
Geomorphic + Land cover	2	42.9
Geomorphic + Aster + Geologic + Land cover	5	46.0
Geomorphic + Aster + Spectral + Geologic + Land cover	4	51.6